

## RESEARCH

# Topmouth culter melanocortin-3 receptor: regulation by two isoforms of melanocortin-2 receptor accessory protein 2

Ren-Lei Ji<sup>1,\*</sup>, Lu Huang<sup>2,\*</sup>, Yin Wang<sup>1</sup>, Ting Liu<sup>1</sup>, Si-Yu Fan<sup>2</sup>, Min Tao<sup>1,2</sup> and Ya-Xiong Tao<sup>1</sup><sup>1</sup>Department of Anatomy, Physiology and Pharmacology, College of Veterinary Medicine, Auburn University, Auburn, Alabama, USA<sup>2</sup>State Key Laboratory of Developmental Biology of Freshwater Fish, College of Life Sciences, Hunan Normal University, Changsha, Hunan, People's Republic of ChinaCorrespondence should be addressed to M Tao or Y-X Tao: [minmindiu@126.com](mailto:minmindiu@126.com) or [taoyaxi@auburn.edu](mailto:taoyaxi@auburn.edu)

\*(R-L Ji and L Huang contributed equally to this work)

## Abstract

Melanocortin-3 receptor (MC3R) is a regulator of energy homeostasis, and interaction of MC3R and melanocortin-2 receptor accessory protein 2 (MRAP2) plays a critical role in MC3R signaling of mammals. However, the physiological roles of MC3R in teleosts are not well understood. In this study, qRT-PCR was used to measure gene expression. Radioligand binding assay was used to study the binding properties of topmouth culter MC3R (caMC3R). Intracellular cAMP generation was determined by RIA, and caMC3R expression was quantified with flow cytometry. We showed that culter *mc3r* had higher expression in the CNS. All agonists could bind and stimulate caMC3R to increase dose dependently intracellular cAMP accumulation. Compared to human MC3R, culter MC3R showed higher constitutive activity, higher efficacies, and  $R_{max}$  to alpha-melanocyte-stimulating hormone ( $\alpha$ -MSH), des- $\alpha$ -MSH, and adrenocorticotrophic hormone. Both caMRAP2a and caMRAP2b markedly decreased caMC3R basal cAMP production. However, only caMRAP2a significantly decreased cell surface expression,  $B_{max}$ , and  $R_{max}$  of caMC3R. Expression analysis suggested that MRAP2a and MRAP2b might be more important in regulating MC3R/MC4R signaling during larval period, and reduced *mc3r*, *mc4r*, and *pomc* expression might be primarily involved in modulation of MC3R/MC4R in adults. These data indicated that the cloned caMC3R was a functional receptor. MRAP2a and MRAP2b had different effects on expression and signaling of caMC3R. In addition, expression analysis suggested that MRAP2s, receptors, and hormones might play different roles in regulating culter development and growth.

## Key Words

- ▶ melanocortin-3 receptor
- ▶ constitutive activity
- ▶ melanocortin-2 receptor accessory protein 2
- ▶ signaling
- ▶ topmouth culter

Endocrine Connections  
(2021) 10, 1489–1501

## Introduction

Melanocortin receptors (MCRs) belong to rhodopsin-like family A G-protein-coupled receptors (GPCRs). Five MCRs (named MC1R–MC5R), with diverse ligand affinities (including  $\alpha$ -,  $\beta$ -,  $\gamma$ -melanocyte-stimulating hormones (MSHs) and adrenocorticotrophic hormone (ACTH)) and multiple physiological roles, have been extensively studied in mammals (1, 2, 3, 4). MC3R and MC4R are known as

neural MCRs with high expression in the CNS (5, 6, 7, 8). These two MCRs play vital roles in modulation of energy homeostasis. Mutations in *MC3R* and *MC4R* are associated with obesity (9, 10, 11). *Mc4r* knockout mice show obesity phenotype with increased food intake and decreased energy expenditure (12, 13). Targeted deletion of *Mc3r* in mice show a moderate obesity phenotype with decreased

lean mass, increased fat mass, normal food intake, and metabolism, suggesting that MC3R could regulate feed efficiency and alterations in nutrient partitioning (14, 15, 16). In addition, studies found that MC3R plays a key role in anomalous metabolic adaption to restricted feeding (17, 18). A recent study showed that MC3R is a critical regulator of boundary controls on melanocortin signaling, providing rheostatic control on energy storage (19).

In addition to the CNS expression, MC3R is also expressed in several peripheral tissues, including the intestine, placenta, heart, gut, kidney, and macrophages (5, 20, 21, 22, 23). Owing to its wide expression, MC3R has been shown to have other potential physiological functions in the periphery, including involvement in immune response and inflammation (20, 23, 24, 25, 26), regulating cardiovascular function (27, 28), and natriuresis (29). The MC3R primarily couples to the stimulatory G protein to stimulate adenyl cyclase activity, leading to increased production of the intracellular second messenger cAMP to trigger downstream signaling.

MCRs have been shown to interact with small single transmembrane proteins – melanocortin-2 receptor accessory proteins (MRAPs, including MRAP1 and MRAP2) (30, 31, 32, 33) (reviewed in (34, 35)). MRAP2 has high expression in CNS and plays a crucial role in regulating energy homeostasis. Targeted deletion of *Mrap2* in mice shows severe obesity (36, 37). MRAP2 interacts with and modulates MC4R signaling in mammals and other species (33, 38, 39, 40, 41, 42). Additionally, the function of MRAP2 in regulating energy homeostasis through MC3R has also been reported (32, 38, 43).

Considering the crucial importance of energy metabolism, understanding the endocrine modulation of energy homeostasis is important for economically important fishes and may potentially lead to novel approaches to manipulate fish growth, feed efficiency, and final product quality in cultured fish. Hence, it is not surprising that MC3R has also attracted some attention in fish. Our mining of NCBI database and literature search revealed that the *mc3r* gene is found in some fish, including Holocephali (elephant shark *Callorhynchus milii*), Elasmobranchii (spiny dogfish *Squalus acanthias*, thorny skate *Amblyraja radiata*, red stingray *Hemirhamphys akajei*, velvet belly lantern shark *Etmopterus spinax*), Polypteriformes (reedfish *Erpetoichthys calabaricus*, gray bichir *Polypterus senegalus*), Lepisosteiformes (spotted gar *Lepisosteus oculatus*), Coelacanth (coelacanth *Latimeria chalumnae*), and teleosts including zebrafish *Danio rerio*, common carp *Cyprinus carpio*, Mexican tetra *Astyanax mexicanus*, red-bellied piranha *Pygocentrus nattereri*, yellow catfish

*Tachysurus fulvidraco*, channel catfish *Ictalurus punctatus*, striped catfish *Pangasianodon hypophthalmus*, electric eel *Electrophorus electricus*, Chinook salmon *Oncorhynchus tshawytscha*, coho salmon *Oncorhynchus kisutch*, river trout *Salmo trutta*, rainbow trout *Oncorhynchus mykiss*, Arctic char *Salvelinus alpinus*, northern pike *Esox lucius*, denticle herring *Denticiceps clupeioides*, and Asian bonytongue *Scleropages formosus*, although it is absent in other species including lungfish *Dipnomorpha*, Acipenseriformes (Yangtze sturgeon *Acipenser dabryanus* and American paddlefish *Polyodon spathula*), cichlid *Simochromis diagramma*, medaka *Oryzias latipes*, fugu *Takifugu rubripes*, stickleback *Gasterosteus aculeatus*, ricefield eel *Monopterus albus*, and orange-spotted grouper *Epinephelus coioides* (39, 44, 45, 46, 47). Since MC3R is considered a specific receptor for  $\gamma$ -MSH in higher vertebrates (5, 7) and  $\gamma$ -MSH is absent in teleosts (48), the absence of MC3R in some fish might be considered as one example of co-evolution of ligand and receptor.

Only three studies have investigated the pharmacological properties of fish MC3Rs so far (43, 44, 49). Of interest, two studies reported high constitutive activities in zebrafish and channel catfish MC3Rs (43, 49), similar to the results in teleost MC4Rs (39, 40, 41, 47, 50, 51, 52, 53) and MC1R (54). In this study, topmouth culter (*Culter alburnus*) was used as an animal model to explore the physiology and pharmacology of culter MC3R. Topmouth culter is an important species of freshwater fish with wide distribution in reservoirs, rivers, and lakes in China (55, 56). We cloned culter *mc3r* and explored its tissue distribution. We also investigated the pharmacology of caMC3R and modulation by caMRAP2s. The potential functions of MC3R, MC4R, and MRAP2s in embryo development and adult were also studied.

## Materials and methods

### Ligands and plasmids

[Nle<sup>4</sup>,D-Phe<sup>7</sup>]- $\alpha$ -MSH (NDP-MSH) was purchased from Peptides International (Louisville, KY, USA). Human  $\alpha$ -MSH was obtained from Pi Proteomics (Huntsville, AL, USA). Human ACTH (1–24) was purchased from Phoenix Pharmaceuticals (Burlingame, CA, USA). Human des-acetyl- $\alpha$ -MSH was obtained from GenScript (Piscataway, NJ, USA). Culter  $\alpha$ -MSH and ACTH are 100 and 87.5% identical with the corresponding human counterparts, respectively (40). [<sup>125</sup>I]-cAMP and [<sup>125</sup>I]-NDP-MSH were iodinated using chloramine T method (57, 58). The human MC3R (hMC3R)

subcloned into pcDNA3.1 vector (pcDNA3.1-hMC3R) was generated as previously described (59). N-terminal Flag-tagged caMRAP2a and N-terminal Flag-tagged caMRAP2b were reported before (40). N-terminal myc-tagged caMC3R was commercially synthesized and subcloned into pcDNA3.1 by GenScript to generate the plasmid used for transfection.

### Animal studies

All animal experiments were approved by Animal Care Committee of Hunan Normal University and was in strict accordance with the Management Rule of Laboratory Animals (Chinese Order No. 676 of the State Council, revised March 1, 2017). Culter were provided and fed in the Engineering Center of Polyploid Fish Breeding of the Ministry of Education (Hunan Normal University, China). After 3 days of acclimation, fish were used for experimentation. Fish were reared in tanks (height of 100 cm and diameter of 95 cm) and fed twice daily at 09:00 and 17:00 h. Experimental conditions were as follows: natural light, water temperature (22–28°C), and dissolved oxygen (approximately 8 mg/L). All fish were anesthetized with MS222 (1:10,000, Sangon Biotech, China) and sampled immediately. Brain was collected and stored at –80°C for RNA extraction and qRT-PCR.

### Gene cloning and sequence alignment

Gene cloning was performed according to the procedure described previously (40). Briefly, total RNA was purified using Trizol™ reagent (Invitrogen). The first-strand cDNA was synthesized using PrimeScript RT reagent kit with gDNA Eraser (TaKaRa). Primers were designed via Primer Premier 5.0 (Supplementary Table 1, see section on [supplementary materials](#) given at the end of this article). PCR products were separated through 1.2% agarose gels, ligated to pMD18-T vector (Takara), and sequenced (Sangon Biotech).

### Tissue distribution of *mc3r*

To explore the tissue distribution of *mc3r*, the mesencephalon, olfactory bulb, cerebellum, telencephalon, medulla, hypothalamus, pituitary gland, muscle, heart, gonads (ovaries and testes), liver, head kidney, spleen, skin, gill, and kidney were collected from three females or males. Three pairs of primers for each gene were designed by AlleleID 6. Each pair of primers was tested for amplification efficiency and melting curve. The primers

were selected in qRT-PCR with 95–105% amplification efficiency and single peak melting curve (Supplementary Table 1). The same trend was found when  $\beta$ -actin, *hprt*, and *gapdh* were used as housekeeping genes to normalize target gene expression. Thus,  $\beta$ -actin was used as the internal reference for normalization in this study. The qRT-PCR was performed using Prism 7500 Sequence Detection System (ABI, Foster City, CA, USA). The amplification was performed in a total volume of 10  $\mu$ L, containing 5  $\mu$ L SYBR green PCR Master Mix, 0.5  $\mu$ L each primer, 3  $\mu$ L water, and 1  $\mu$ L cDNA. The RT-qPCR program was set as follows: 50°C for 2 min, 95°C for 10 min, followed by 40 cycles at 95°C for 15 s and 61°C for 45 s. Each sample was added to a 96-well plate repeated thrice. The relative expression of genes was calculated using the  $2^{-\Delta\Delta CT}$  method (60).

### Cell culture and transfection

Human embryonic kidney (HEK) 293T cells (ATCC) were cultured in an incubator (37°C in a 5% CO<sub>2</sub>-humidified atmosphere) (61). Briefly, the medium contained Dulbecco's Modified Eagle's medium (Invitrogen), 10% newborn calf serum, 0.25  $\mu$ g/mL of amphotericin B, 100 IU/mL of penicillin, 100  $\mu$ g/mL streptomycin, 50  $\mu$ g/mL of gentamicin, and 10 mM HEPES. Cells were plated into 6-well or 24-well plates pre-coated with 0.1% gelatin. At approximately 70% confluency, cells were transfected with 0.25  $\mu$ g/ $\mu$ L MC3R with or without MRAP2 plasmids using calcium phosphate precipitation method (62). Empty vector pcDNA3.1 was used to normalize the total DNA in each well.

### Flow cytometry assay

The expression of the caMC3R was quantified with flow cytometry as described earlier (53, 63), carried out by the C6 Accuri Cytometer (Accuri Cytometers, Ann Arbor, MI, USA). Four ratios (1:0, 1:1, 1:3, and 1:5) of caMC3R and caMRAP2a/caMRAP2b plasmids were co-transfected into cells in six-well plates. Fluorescence of cells transfected with empty vector (pcDNA3.1) was used for background staining. The expression of the caMC3R was calculated as the percentage of 1:0 group was set as 100% expression. The expression levels of other groups were calculated as % of the 1:0 group (63).

### Ligand binding assays

Binding assay was described previously (43, 61). The ligands and their final concentrations used in this study

were NDP-MSH (from  $10^{-12}$  to  $10^{-6}$  M),  $\alpha$ -MSH (from  $10^{-12}$  to  $10^{-6}$  M), des-acetyl- $\alpha$ -MSH (from  $10^{-12}$  to  $10^{-6}$  M), or ACTH (1–24) (from  $10^{-12}$  to  $10^{-6}$  M). To investigate the modulation of caMRAP2a or caMRAP2b on the binding property of caMC3R, caMC3R (0.25  $\mu\text{g}/\mu\text{L}$ ) and caMRAP2a or caMRAP2b plasmids in two ratios (1:0 and 1:5) were applied to co-transfect cells (six-well plate), and ACTH (1–24) (from  $10^{-11}$  to  $10^{-6}$  M) and  $\alpha$ -MSH (from  $10^{-10}$  to  $10^{-5}$  M) were used.

### cAMP assays

cAMP signaling assay was performed as described previously (57, 61). The final concentration of ligands used was  $10^{-12}$  to  $10^{-6}$  M. To explore the effects of caMRAP2a and caMRAP2b on caMC3R signaling, cells (24-well plate) were transfected with caMC3R (0.25  $\mu\text{g}/\mu\text{L}$ ) and caMRAP2a or caMRAP2b plasmids in two ratios (1:0 and 1:5), and two

ligands,  $\alpha$ -MSH (from  $10^{-13}$  to  $10^{-7}$  M) and ACTH (1–24) (from  $10^{-13}$  to  $10^{-7}$  M) were used. To investigate the dose-dependent modulation of caMRAP2a or caMRAP2b on maximal response ( $R_{\text{max}}$ ) of cAMP signaling of caMC3R to  $\alpha$ -MSH stimulation ( $10^{-6}$  M), four ratios (1:0, 1:1, 1:3, and 1:5) of caMC3R (0.25  $\mu\text{g}/\mu\text{L}$ ) and caMRAP2a or caMRAP2b were co-transfected into cells (24-well plate). To study the constitutive activity of cAMP signaling, caMC3R plasmid in increasing concentrations (0, 0.007, 0.015, 0.030, 0.060, 0.125, and 0.250  $\mu\text{g}/\mu\text{L}$ ) were transfected into cells (six-well plate).

### Physiological functions in the embryos and adults

To explore the roles of MC3R, MC4R, and MRAP2s in the embryo development and adult brain, the embryos at 1, 2, 3, 4, and 5 days post-fertilization (dpf) and the brain of adult culter in different weights ( $20.02 \pm 1.38$  g,  $50 \pm 3.25$  g,

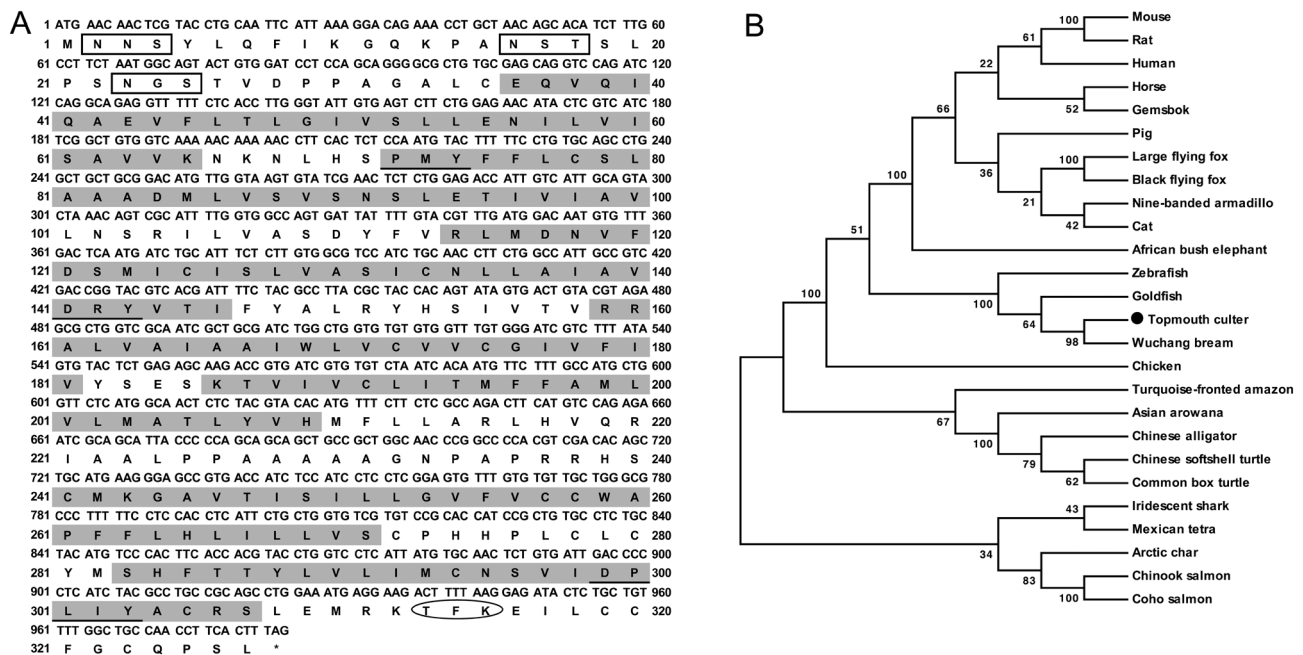


**Figure 1**

Nucleotide and deduced amino acid sequences (A) and phylogenetic tree (B) of caMC3R. Positions of nucleotide and amino acid sequences are indicated on both sides. N-linked glycosylation sites are present in open boxes. Shaded boxes show putative TMD1–7. Oval frame denotes potential phosphorylation site. The conserved motifs (PMY, DRY, and DPxxY) are underlined. Asterisk (\*) shows stop codon. The tree was constructed by the neighbor-joining method. Numbers at nodes indicate the bootstrap value, as percentages, obtained for 1000 replicates. Black dot denotes culter MC3R. MC3Rs: *Culter alburnus* (topmouth culter, MW419813), *Megalobrama amblycephala* (Wuchang bream, AWA81517.1), *Carassius auratus* (goldfish, BAJ83473.1), *Danio rerio* (zebrafish, AAO24744.1), *Oncorhynchus kisutch* (coho salmon, XP\_020360426.1), *Homo sapiens* (human, NP\_063941.3), *Mus musculus* (mouse, AA103670.1), *Gallus gallus* (chicken, XP\_004947293.1), *Sus scrofa* (pig, AFK25142.1), *Rattus norvegicus* (rat, NP\_001020441.3), *Equus caballus* (horse, NP\_001243901.1), *Pangasianodon hypophthalmus* (iridescent shark, XP\_026770221.1), *Astyanax mexicanus* (Mexican tetra, XP\_007231215.1), *Oryx gazella* (gemsbok, AFH58734.1), *Pteropus vampyrus* (large flying fox, XP\_011368476.1), *Pteropus alecto* (black flying fox, XP\_006921991.1), *Dasyatis novemcinctus* (nine-banded armadillo, XP\_004447768.1), *Felis catus* (cat, XP\_023106851.1), *Loxodonta africana* (African bush elephant, XP\_003419952.1), *Oncorhynchus tshawytscha* (chinook salmon, XP\_024229914.1), *Salvelinus alpinus* (Arctic char, XP\_023994975.1), *Amazona aestiva* (turquoise-fronted amazon, KQL61336.1), *Scleropages formosus* (Asian arowana, XP\_018615783.1), *Pelodiscus sinensis* (Chinese softshell turtle, XP\_006129463.1), *Terrapene carolina triunguis* (common box turtle, XP\_024059166.1), and *Alligator sinensis* (Chinese alligator, XP\_006018246.1).



100 ± 8.12 g, 200 ± 13.81 g, 500 ± 30.56 g, and 800 ± 40.93 g) were obtained. Each stage had at least three fish.

### Statistical analysis

All data were shown as mean ± s.e.m. GraphPad Prism 8.3 software (GraphPad) was used to calculate the parameters of ligand binding and cAMP signaling assays. The significance of differences in expression levels, ligand binding, and cAMP signaling parameters between caMC3R and hMC3R, as well as vehicle and ligand-treated groups, were all determined by Student's *t*-test. *F* test was first analyzed to compare variances for each study. If *P* value for *F* test is less than 0.05, an unpaired *t*-test with Welch's correction would be performed. If *P* value for *F* test is more than 0.05, a normal unpaired *t*-test would be performed.

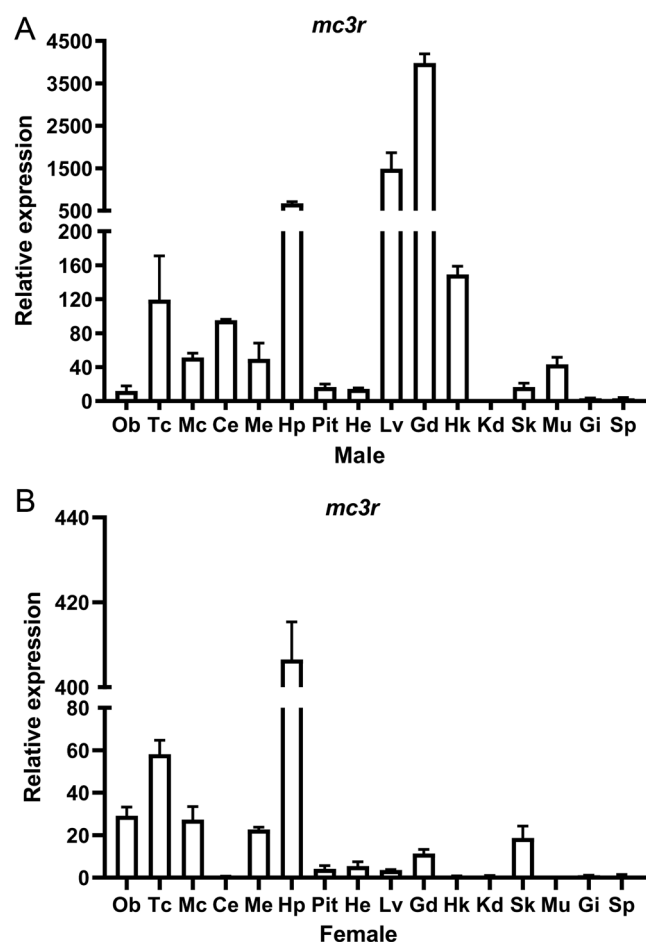


**Figure 2** Tissue expression of *mc3r* in male (A) and female (B) culter. The mRNA levels of *mc3r* were measured by qRT-PCR. Data are presented as the mean ± s.e.m. (*n* = 3). Mc: mesencephalon; Ob: olfactory bulb; Ce: cerebellum; Tc: telencephalon; Hp: hypothalamus; Me: medulla; Pit: pituitary gland; Lv: liver; He: heart; St: stomach; Kd: kidney; Int: intestine; Hk: head kidney; Gd: gonad; Mu: muscle; Sk: skin; Gi: gill; Sp: spleen.

One-way ANOVA was used to analyze the significance of differences in binding, cAMP, flow cytometry, and gene expression between multiple groups. For one-way ANOVA (more than two groups), if *P* value for *F* test is less than 0.05, the transformation would be performed to meet the *P* value for *F* test. Statistical significance was set at *P* < 0.05.

## Results

### Nucleotide and deduced amino acid sequences of caMC3R

The cloned culter *mc3r* (GenBank: MW419813) had a 984-bp open reading frame, encoding a protein of 327 amino acids with an estimated molecular mass of 36.01 kDa (Fig. 1A). Multiple alignment of MC3Rs revealed that the predicated caMC3R had the classical characteristic of Family A GPCRs, with seven hydrophobic transmembrane domains (TMDs) and several conserved motifs (PMY, DRY, and DPxxY) at homologous positions with MC3Rs of other species (Supplementary Fig. 1). Three potential N-linked glycosylation sites (Asn<sup>2</sup>, Asn<sup>16</sup>, and Asn<sup>23</sup>) in N-terminus and consensus sequence for protein kinase C phosphorylation (Thr<sup>313</sup>Phe<sup>314</sup>Lys<sup>315</sup>) in the C-terminus were found in caMC3R (Fig. 1A). The identities between caMC3R and other piscine MC3R orthologs were 99% to Wuchang bream, 98% to goldfish, 97% to common carp, 95% to zebrafish, 81% to coho salmon, as well as high homology to mammalian MC3Rs (with 83% to pig and mouse and 82% to human) (Supplementary Fig. 1). Phylogenetic tree showed that caMC3R nested with Wuchang bream, goldfish, and zebrafish MC3Rs (Fig. 1B).

### Tissue distribution of culter *mc3r*

The tissue distribution of culter *mc3r* was determined by qRT-PCR (Fig. 2). Culter *mc3r* expression showed sexual dimorphism. In male culter, *mc3r* was primarily expressed in the brain, including telencephalon, cerebellum, medulla, mesencephalon, and hypothalamus, as well as highly expressed in the periphery (testis, liver, and head kidney) (Fig. 2A). In female culter, *mc3r* was highly expressed in the telencephalon, olfactory bulb, medulla, mesencephalon, and hypothalamus and also expressed in skin and ovary (Fig. 2B).

### Ligand binding properties of caMC3R

Binding assay was performed using multiple MC3R ligands, including NDP-MSH, α-MSH, des-α-MSH, and

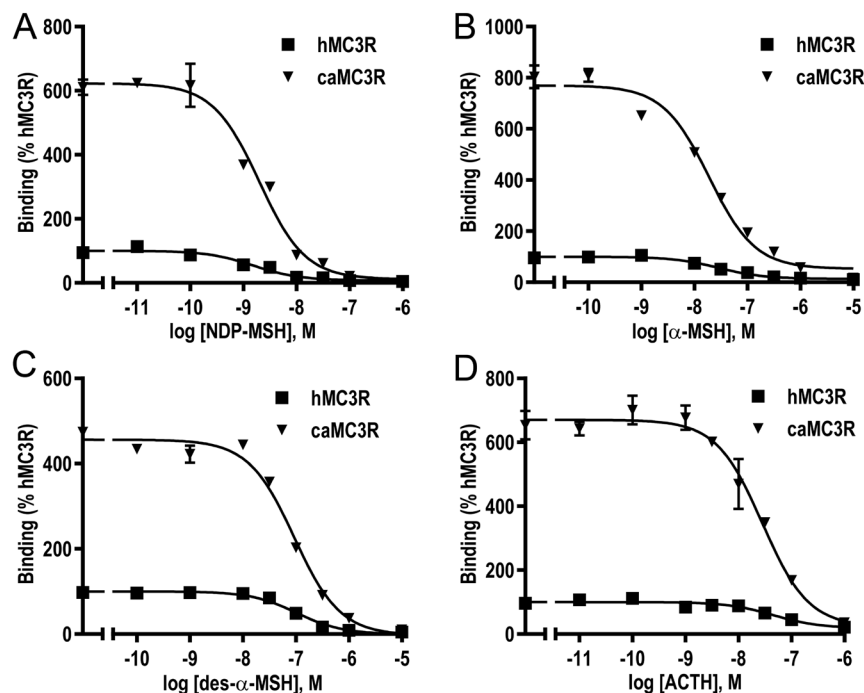


**Figure 3** Ligand binding properties of caMC3R. Different concentrations of unlabeled NDP-MSH (A),  $\alpha$ -MSH (B), des- $\alpha$ -MSH (C), and ACTH (1–24) (D) were used to displace the binding of  $^{125}$ I-NDP-MSH. Results are expressed as % of hMC3R binding  $\pm$  range from duplicate determinations within one experiment. All experiments were repeated at least three independent times.

ACTH (1–24). hMC3R was used for comparison in the same experiments. The maximal binding value ( $B_{max}$ ) of caMC3R was  $627.02 \pm 68.52\%$  of that of the hMC3R (set as 100%) ( $P < 0.001$ ) (Fig. 3 and Table 1). caMC3R had significantly higher affinity to ACTH (1–24) ( $P < 0.05$ ) (Fig. 3 and Table 1).  $IC_{50}$ s were similar between the two MC3Rs when NDP-MSH,  $\alpha$ -MSH, or des- $\alpha$ -MSH was used (Fig. 3 and Table 1).

### cAMP signaling properties of caMC3R

cAMP signaling properties were measured to investigate whether caMC3R could respond to NDP-MSH,  $\alpha$ -MSH, des- $\alpha$ -MSH, or ACTH (1–24) stimulation. The results indicated that all agonists could stimulate caMC3R and dose dependently increase intracellular cAMP generation (Fig. 4 and Table 2). caMC3R had higher maximal responses ( $R_{max}$ ) to all agonists than those of hMC3R (Fig. 4 and Table 2).  $EC_{50}$ s were remarkably decreased when

caMC3R was stimulated by ACTH (1–24) and des- $\alpha$ -MSH (Fig. 4 and Table 2).

This study also showed that caMC3R had four times higher basal cAMP levels than that of hMC3R (Table 2). To further study whether caMC3R could be constitutively active, increasing concentrations (from 0 to 0.25  $\mu$ g/ $\mu$ L) of caMC3R plasmid were transfected into cells. The data indicated that a low amount of caMC3R plasmid transfection could increase basal cAMP signaling, starting at 0.03  $\mu$ g/ $\mu$ L (Fig. 4E).

### Regulation of caMC3R expression and pharmacology by caMRAP2s

This study and our previous study showed that the mRNA of culter *mc3r*, *mrp2a*, and *mrp2b* was detected in the same tissues (40), indicating that MRAP2s might affect MC3R pharmacology. Therefore, we further investigated the potential modulation of caMRAP2s on MC3R expression and pharmacology.

Flow cytometry was used to measure caMC3R expression. We found that caMRAP2a significantly decreased the cell surface expression in 1:5 group but had no effect on total expression of caMC3R (Fig. 5A and B). However, caMRAP2b did not significantly affect the cell surface and total expression of caMC3R (Fig. 5A and B).

Ligand binding assays with  $\alpha$ -MSH and ACTH indicated that only caMRAP2a significantly decreased the  $B_{max}$  of caMC3R in 1:5 group, but caMRAP2b did not (Fig. 6A, B

**Table 1** The ligand binding properties of caMC3R.

MC3R		caMC3R	hMC3R
$B_{max}$ (%)		$627.02 \pm 68.52^b$	100
NDP-MSH	$IC_{50}$ (nM)	$2.78 \pm 0.71$	$1.78 \pm 0.15$
$\alpha$ -MSH	$IC_{50}$ (nM)	$20.81 \pm 3.88$	$30.73 \pm 1.31$
des- $\alpha$ -MSH	$IC_{50}$ (nM)	$123.97 \pm 11.48$	$117.95 \pm 14.72$
ACTH (1–24)	$IC_{50}$ (nM)	$19.66 \pm 5.58^a$	$43.61 \pm 3.44$

Results are presented as the mean  $\pm$  s.e.m. ( $n = 3-4$ ).

<sup>a</sup>Significant difference from the parameter of hMC3R,  $P < 0.05$ . <sup>b</sup>Significant difference from the parameter of hMC3R,  $P < 0.001$ .

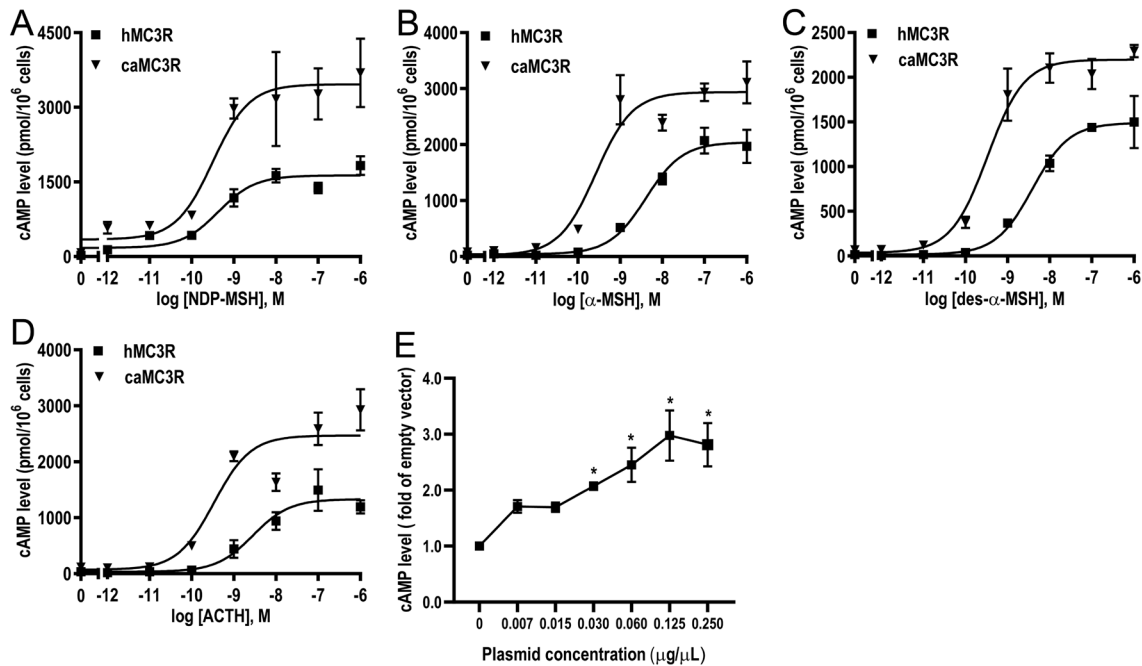


**Figure 4**

Signaling properties of caMC3R. HEK293T cells were transiently transfected with hMC3R or caMC3R plasmids. Different concentrations of NDP-MSH (A),  $\alpha$ -MSH (B), des- $\alpha$ -MSH (C), and ACTH (1–24) (D) were used to stimulate the cells. (E) Constitutive activities of caMC3R in cAMP pathway. Increasing concentrations of caMC3R plasmid were transfected into HEK293T cells. Cells transfected with empty pcDNA3.1 vector were used as the control group. Data are mean  $\pm$  s.e.m. from triplicate measurements within one experiment. All experiments were performed at least three times independently.

and Table 3). caMRAP2a and caMRAP2b had no significant effect on affinities of caMC3R to  $\alpha$ -MSH and ACTH (1–24) (Fig. 6A, B and Table 3).

Modulation of caMRAP2a or caMRAP2b on caMC3R signaling was also studied. Results showed that both MRAP2a and MRAP2b did not markedly affect  $EC_{50}$ s in response to  $\alpha$ -MSH and ACTH; MRAP2a significantly decreased  $R_{max}$ , but MRAP2b did not (Fig. 6C, D and Table 4). Additionally, increasing ratios of caMC3R/caMRAP2a or caMRAP2b (1:0, 1:1, 1:3, and 1:5) were co-transfected into cells. Results showed that both MRAP2a and MRAP2b dose dependently decreased basal cAMP generation (Fig. 5C). The cAMP generation of caMC3R stimulated by  $10^{-6}$  M  $\alpha$ -MSH were dose dependently decreased by MRAP2a but not MRAP2b (Fig. 5D).

### Expression of *mc3r*, *mc4r*, *mrap2a*, and *mrap2b* in culter embryos and adults

qRT-PCR was used to analyze developmental expression kinetics of *pomc*, *argp*, *mc3r*, *mc4r*, *mrap2a*, and *mrap2b* in the culter embryo at 1, 2, 3, 4, or 5 dpf. All genes could be detected from 1 dpf to 5 dpf (Fig. 7). Compared to 1 dpf, expression of *pomc*, *mc4r* and *mrap2a* was increased at 3, 4,

or 5 dpf; *argp* and *mc3r* expression was decreased at 2, 3, 4, or 5 dpf (Fig. 7).

In adult culter, brains were collected from fish of different weights. Results showed that with increasing weight, expression of *argp*, *mc3r*, *mc4r*, and *mrap2a* decreased (Fig. 8B, C, D and E). Compared to ~20 g fish, *pomc* expression was significantly increased at ~50 g and then decreased at ~500 and 800 g (Fig. 8A). Expression of *mrap2b* was markedly increased at ~50 g and ~800 g and decreased at ~500 g (Fig. 8F).

**Table 2** The signaling properties of caMC3R.

MC3R		caMC3R	hMC3R
Basal (%)		406.89 $\pm$ 50.49 <sup>c</sup>	100
NDP-MSH	$EC_{50}$ (nM)	0.42 $\pm$ 0.13	0.28 $\pm$ 0.08
	$R_{max}$ (%)	208.87 $\pm$ 15.15 <sup>a</sup>	100
$\alpha$ -MSH	$EC_{50}$ (nM)	0.22 $\pm$ 0.04	1.70 $\pm$ 0.42
	$R_{max}$ (%)	171.91 $\pm$ 15.40 <sup>a</sup>	100
des- $\alpha$ -MSH	$EC_{50}$ (nM)	0.29 $\pm$ 0.05 <sup>a</sup>	3.14 $\pm$ 0.38
	$R_{max}$ (%)	168.17 $\pm$ 11.07 <sup>a</sup>	100
ACTH (1–24)	$EC_{50}$ (nM)	0.44 $\pm$ 0.12 <sup>b</sup>	4.82 $\pm$ 0.79
	$R_{max}$ (%)	140.92 $\pm$ 7.05 <sup>a</sup>	100

Results are presented as the mean  $\pm$  s.e.m. ( $n = 3-4$ ).

<sup>a</sup>Significant difference from the parameter of hMC3R,  $P < 0.05$ . <sup>b</sup>Significant difference from the parameter of hMC3R,  $P < 0.01$ . <sup>c</sup>Significant difference from the parameter of hMC3R,  $P < 0.001$ .

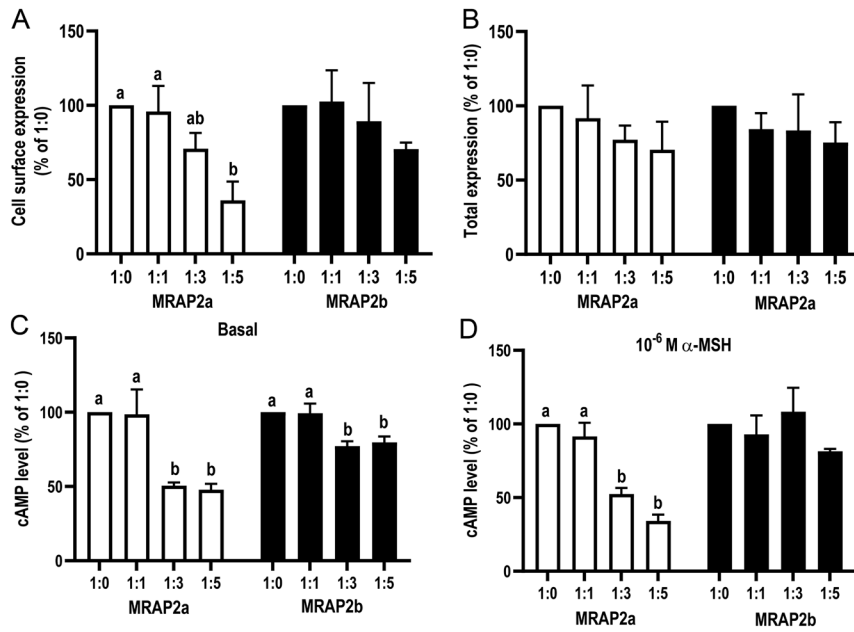


**Figure 5**

Regulation of caMC3R expression and signaling by caMRAP2a or caMRAP2b. Cell surface expression (A) and total expression (B) of caMC3R modulated by caMRAP2a or caMRAP2b were measured by flow cytometry. Basal (C) and maximal signaling (D) of caMC3R regulated by MRAP2a or MRAP2b were determined by RIA. HEK293T cells were co-transfected with different ratios of caMC3R/caMRAP2a or caMC3R/caMRAP2b (1:0, 1:1, 1:3, and 1:5). The empty vector pcDNA3.1 fluorescence was used for background staining. The results are calculated as % of 1:0 group. Each data point represented as the mean ± s.e.m. ( $n = 3 - 4$ ). Different letters indicate significant difference ( $P < 0.05$ ) (one-way ANOVA followed by Tukey test).

## Discussion

In this study, we cloned culter *mc3r* and explored the pharmacological properties of caMC3R and its modulation by MRAP2a and MRAP2b. The expression of *mc3r*, *mc4r*, *mrp2a*, and *mrp2b* in embryos and adults was further investigated.

Culter *mc3r* had similar primary structure as MC3Rs of other species with seven TMDs and several highly conserved motifs (Supplementary Fig. 1). Phylogenetic tree analysis found that caMC3R was clustered with teleost MC3Rs (Fig. 1B). Culter *mc3r* was primarily

expressed in the brain (Fig. 2). Differential expression patterns were observed in peripheral organs between the sexes. In males, culter *mc3r* was highly expressed in peripheral tissues, including liver, muscle, testis, and head kidney, whereas it was highly expressed in skin, ovary, and liver in females (Fig. 2). In chicken, *mc3r* mRNA is detected in the brain, muscle, and ovary (38). In red stingray, *mc3r* has high expression in the brain and inter-renal tissues (64). The wide expression (in the brain and peripheral tissues) of *mc3r* might be associated with its roles in regulating multiple physiological functions, including modulation of feed efficiency and nutrient

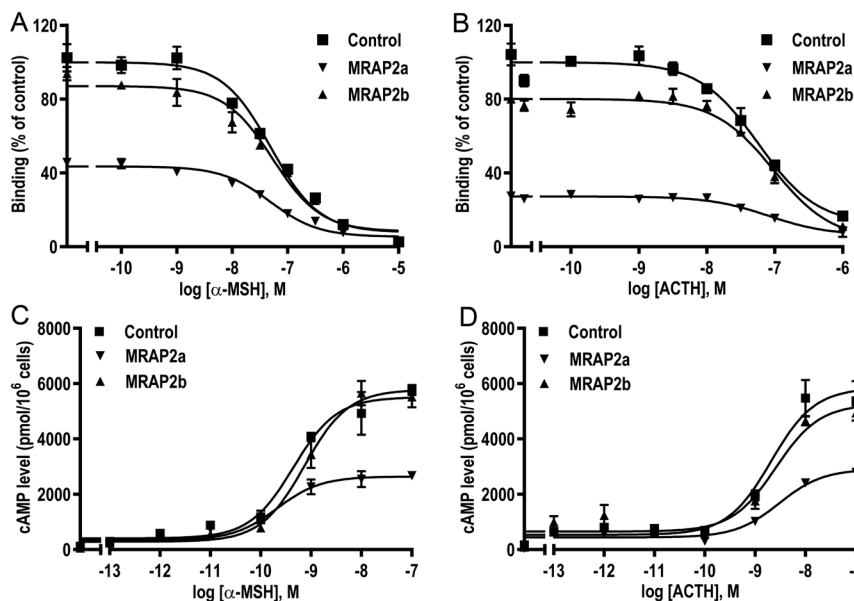


**Figure 6**

Modulation of caMC3R pharmacology by caMRAP2a or caMRAP2b. Ligand binding (A, B) and signaling (C, D) properties of caMC3R to α-MSH or ACTH (1–24) upon co-expression of caMC3R with caMRAP2a or caMRAP2b were measured. HEK293T cells were co-transfected with caMC3R/caMRAP2a or caMC3R/caMRAP2b in two different ratios (1:0 and 1:5). Results of binding properties were calculated as % of hMC3R binding ± range from duplicate determinations within one experiment. All experiments were measured at least three times independently.



**Table 3** The effect of caMRAP2a or caMRAP2b on ligand binding properties of caMC3R.

caMC3R/caMRAP2s	$B_{max}$	$\alpha$ -MSH, $IC_{50}$ (nM)	ACTH, $IC_{50}$ (nM)
caMC3R/caMRAP2 (1:0)	100	40.97 ± 8.63	83.73 ± 13.89
caMC3R/caMRAP2a (1:5)	48.71 ± 5.03 <sup>a</sup>	33.97 ± 7.18	57.43 ± 12.43
caMC3R/caMRAP2b (1:5)	86.57 ± 6.61	49.20 ± 2.97	107.13 ± 27.48

Results are expressed as the mean ± s.e.m. ( $n = 3-4$ ).

<sup>a</sup>Significant difference from the parameter of 1:0,  $P < 0.001$ .

partitioning, adaptation to fasting and overfeeding, as well as immune response.

Detailed pharmacological studies were performed on culter MC3R. Results showed that all agonists could bind and activate caMC3R (Figs 3 and 4). We found that caMC3R had high affinity and potency to ACTH (Tables 1 and 2), similar to dogfish (44) and channel catfish (43) MC3Rs. Fish MC4Rs also show high affinities and potencies to ACTH (40, 47, 51, 52, 65, 66). These indicated that ACTH may be the original ligand for the MC3R and MC4R (67). In addition, caMC3R showed decreased  $EC_{50}$ s than hMC3R in response to  $\alpha$ -MSH, des- $\alpha$ -MSH, and ACTH (Fig. 4 and Table 2). These results were similar to those of channel catfish MC3R (ipMC3R) where ipMC3R shows a significant decrease of  $EC_{50}$ s in response to  $\alpha$ -MSH and ACTH (43). In addition, caMC3R has higher  $R_{max}$ s than that of hMC3R to all agonist (Fig. 4 and Table 2). In channel catfish, MC3R shows lower  $R_{max}$ s than that of hMC3R to NDP-MSH,  $\alpha$ -MSH,  $\beta$ -MSH, and ACTH (43).

We further explored the potential modulation of the trafficking, ligand binding, and signaling on caMC3R by caMRAP2s. Culter MRAP2a decreased cell surface expression but had no effect on total expression of caMC3R, and MRAP2b did not affect cell surface and total expression of caMC3R (Fig. 5). Both human MRAP1a and MRAP2 do not significantly affect hMC3R cell surface expression (32, 68). Zhang *et al.* showed that MRAP1 and MRAP2 have no effect on the cell surface expression of chicken MC3R (38). Collectively, the potential roles of MRAPs on MC3R cell surface expression vary in different species.

In this study, we also showed that MRAP2a and MRAP2b did not affect affinities of caMC3R to  $\alpha$ -MSH and ACTH (Fig. 6A, B and Table 3). MRAP2a decreased

the  $B_{max}$  of caMC3R, probably due to decreased cell surface expression. As for signaling, both MRAP2a and MRAP2b significantly decreased caMC3R basal activity (Fig. 5C), and only MRAP2a markedly decreased the  $R_{max}$  (Table 4). Similar results were observed in channel catfish MC3R that MRAP2 decreases basal and ligand-stimulated cAMP signaling (43). In zebrafish, MRAP2a and MRAP2b do not modulate MC3R signaling (33). In hMC3R, MRAP2 significantly decreases NDP-MSH-induced cAMP generation, and MRAP1a increases agonist-stimulated cAMP signaling (32, 68). In chicken, MRAP2 increases agonist-induced cAMP production and reduces constitutive activity of MC3R, while MRAP1 has no effect on basal and agonist-induced cAMP generation (38). Furthermore, MRAP1 and MRAP2 increase sensitivity to ACTH of chicken MC3R (38). MRAP2a increases the sensitivity of zebrafish MC4R to ACTH (69, 70). MRAP2 also increases ACTH potency and makes hMC4R act as an ACTH-preferring receptor (69). However, this study and our previous reports on grouper MC4R do not find that MRAP2s could make MC3R or MC4R act as ACTH-preferring receptor (39, 40).

Our results demonstrated that caMC3R had high constitutive activity in cAMP signaling (Fig. 4 and Table 2), consistent with zebrafish, channel catfish, and chicken MC3Rs (38, 43, 49). The high basal activities of MC3R were decreased by MRAP2s in culter, channel catfish, and chicken (38, 43). AgRP (Agouti-related peptide), as an inverse agonist, decreases the constitutive activity of MC3R in channel catfish and chicken (38, 43). However, hMC3R has little or no basal activity in cAMP pathway (71, 72). hMC4R shows modest constitutive activity, and the defect in basal activity of MC4R mutations is

**Table 4** The effect of caMRAP2a or caMRAP2b on cAMP signaling of caMC3R.

caMC3R/caMRAP2a or caMRAP2b	$\alpha$ -MSH		ACTH	
	$EC_{50}$ (nM)	$R_{max}$	$EC_{50}$ (nM)	$R_{max}$
caMC3R (1:0)	0.41 ± 0.02	100	2.09 ± 0.17	100
caMC3R/caMRAP2a (1:5)	0.29 ± 0.04	50.86 ± 7.13 <sup>b</sup>	1.91 ± 0.57	42.49 ± 9.45 <sup>a</sup>
caMC3R/caMRAP2b (1:5)	0.57 ± 0.15	111.62 ± 6.28	1.87 ± 0.38	99.36 ± 13.22

Results are expressed as the mean ± s.e.m. ( $n = 3-4$ ).

<sup>a</sup>Significant difference from the parameter of 1:0,  $P < 0.05$ . <sup>b</sup>Significant difference from the parameter of 1:0,  $P < 0.001$ .

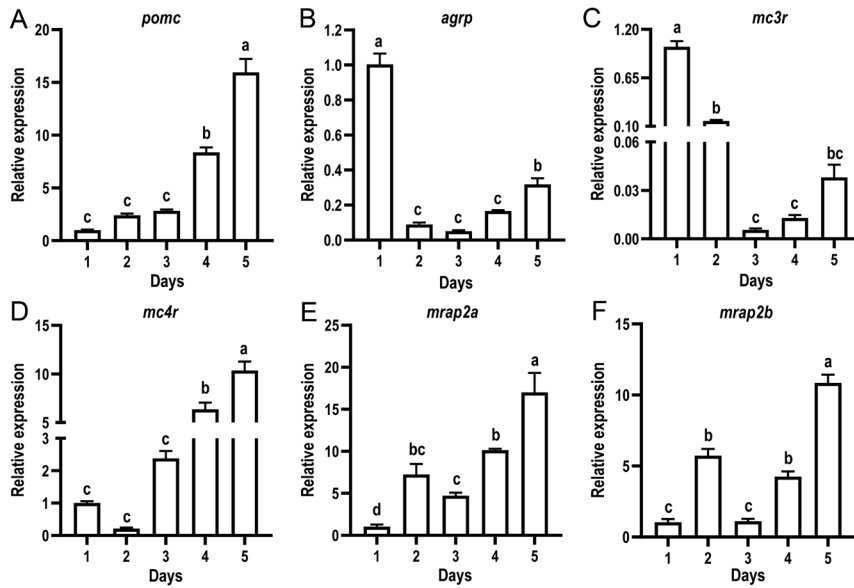


**Figure 7** Expression of *pomc* (A), *agrp* (B), *mc3r* (C), *mc4r* (D), *mrap2a* (E), and *mrap2b* (F) in the first 5 days of culter embryos. Results are expressed as means  $\pm$  s.e.m. ( $n = 3$ ) and are analyzed by one-way ANOVA followed by Tukey's test. Bars with the same letter are not significantly different ( $P > 0.05$ ).

considered as one cause of obesity (73, 74). MRAP2- and AgRP-suppressed basal activity of MC4R is essential for promoting zebrafish growth (33, 75). Thus, high basal activity of MC3R might provide new strategies to modulate MC3R signaling by AgRP or MRAP2 in these species. The potential physiological relevance of constitutive activity in teleost MC3Rs needs further study.

We next explored the potential roles of MC3R, MC4R, and MRAP2s in culter embryo development and adults. Sebag *et al.* reported that zebrafish MRAP2a (expressed from embryos to adults) stabilizes MC4R in an inactive conformation, decreases basal and ligand-stimulated signaling, and maximizes growth during the embryo period. MRAP2b is mainly expressed in adults, reducing

basal activity and enhancing sensitivity of MC4R to agonist, and thus converting constitutive MC4R to ligand-dependent receptor (33). Similar to our previous study on caMC4R (40), this study showed that caMC3R had high basal activity; MRAP2a decreased basal and agonist-stimulated signaling, and MRAP2b only decreased basal activity of caMC3R. Our study showed that increased *mrap2a* and *mrap2b* expression was observed in culter embryos (Fig. 7) and might contribute to inhibit caMC3R and caMC4R signaling and thus maximize growth. In addition, culter *mc3r* had the highest expression at 1 dpf, but lower expression on other dpfs (Fig. 7), indicating that MC3R might lower its signaling by reducing its expression and further promoting growth. In adult culter, expression

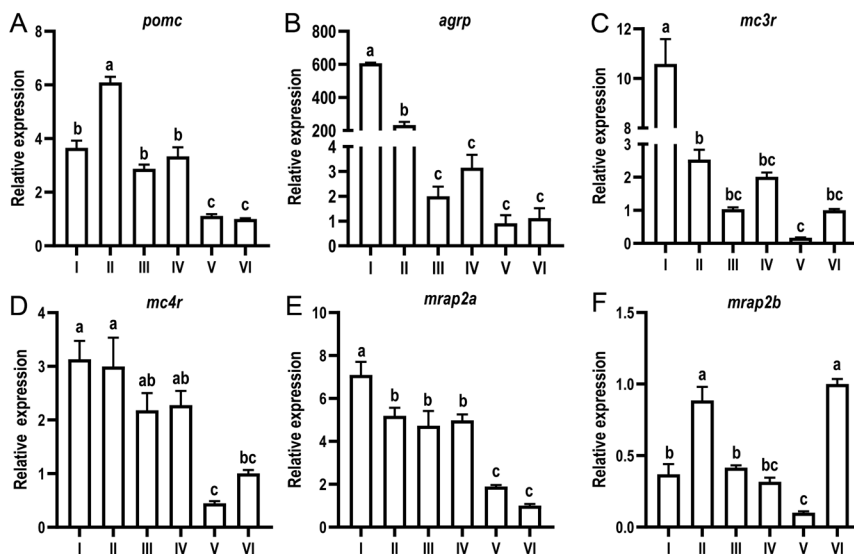


**Figure 8** Expression of *pomc* (A), *agrp* (B), *mc3r* (C), *mc4r* (D), *mrap2a* (E), and *mrap2b* (F) in the brain of adult culter. I, II, III, IV, V, and VI indicated culter of different weights, at  $20.02 \pm 1.38$  g,  $50 \pm 3.25$  g,  $100 \pm 8.12$  g,  $200 \pm 13.81$  g,  $500 \pm 30.56$  g, and  $800 \pm 40.93$  g, respectively. Results are expressed as means  $\pm$  s.e.m. ( $n = 3$ ) and are analyzed by one-way ANOVA followed by Tukey's test. Bars with the same letter are not significantly different ( $P > 0.05$ ).

of *pomc*, *mc3r*, and *mc4r* was gradually decreased (Fig. 8). Lower *mc4r* expression, decreased stimulation by  $\alpha$ -MSH/ACTH would reduce the anorexic action of MC4R, and further promoting food intake and rapid growth. Furthermore, decreased *mc3r* expression and ligand-induced signaling of MC3R might also affect feed efficiency and nutrient partitioning and further improve growth. Overall, MRAP2a and MRAP2b could block MC3R/MC4R functions and promote growth during larval period. Inhibition of MC3R and MC4R signaling by reduced *m3cr*, *mc4r*, and *pomc* expression would affect feeding, feed efficiency, and nutrient partitioning and further maximize growth in adults.

In summary, we cloned culter *mc3r* and investigated its expression patterns. Culter MC3R had high constitutive activity in cAMP pathway. Only caMRAP2a markedly decreased cell surface expression and  $R_{max}$  of caMC3R. Both caMRAP2a and caMRAP2b decreased basal cAMP production. MRAP2a and MRAP2b might play a more important role in regulating MC3R/MC4R signaling during larval period. Reduced expression of *mc3r*, *mc4r*, and *pomc* might be mainly involved in adults. These findings laid the foundation for further physiological studies of culter MC3R that might provide new strategies for promoting growth and culture of culter.

#### Supplementary materials

This is linked to the online version of the paper at <https://doi.org/10.1530/EC-21-0459>.

#### Declaration of interest

The authors declare that there is no conflict of interest that could be perceived as prejudicing the impartiality of the research reported.

#### Funding

This work was supported by the National Natural Science Foundation of China (Grant No. 31872551), the Natural Science Foundation of Hunan Province for Distinguished Young Scholars (Grant No. 2020JJ2022), 111 Project (D20007), and the China Agriculture Research System (Grant No. CARS-45) (to Min Tao). This study was also partially supported by Ocean University of China-Auburn University Joint Center Grants Program (to Ya-Xiong Tao). Ren-Lei Ji, Ting Liu, and Min Tao received fellowships from China Scholarship Council, People's Republic of China.

#### Author contribution statement

Ren-Lei Ji: Writing – Original draft, Data curation, Methodology. Lu Huang: Data curation, Methodology, Formal analysis. Yin Wang: Software, Data curation, Methodology. Ting Liu: Software, review and editing. Si-Yu Fan: Methodology, Formal analysis. Min Tao: Project administration, Validation, Funding acquisition. Ya-Xiong Tao: Supervision, Funding acquisition, Conceptualization, Writing – review and editing.

## References

- Smith AI & Funder JW. Proopiomelanocortin processing in the pituitary, central nervous system, and peripheral tissues. *Endocrine Reviews* 1988 **9** 159–179. (<https://doi.org/10.1210/edrv-9-1-159>)
- Gantz I & Fong TM. The melanocortin system. *American Journal of Physiology: Endocrinology and Metabolism* 2003 **284** E468–E474. (<https://doi.org/10.1152/ajpendo.00434.2002>)
- Cone RD. Studies on the physiological functions of the melanocortin system. *Endocrine Reviews* 2006 **27** 736–749. (<https://doi.org/10.1210/er.2006-0034>)
- Tao YX. Melanocortin receptors. *Biochimica et Biophysica Acta: Molecular Basis of Disease* 2017 **1863** 2411–2413. (<https://doi.org/10.1016/j.bbadis.2017.08.001>)
- Gantz I, Konda Y, Tashiro T, Shimoto Y, Miwa H, Munzert G, Watson SJ, DelValle J & Yamada T. Molecular cloning of a novel melanocortin receptor. *Journal of Biological Chemistry* 1993 **268** 8246–8250. ([https://doi.org/10.1016/S0021-9258\(18\)53088-X](https://doi.org/10.1016/S0021-9258(18)53088-X))
- Gantz I, Miwa H, Konda Y, Shimoto Y, Tashiro T, Watson SJ, DelValle J & Yamada T. Molecular cloning, expression, and gene localization of a fourth melanocortin receptor. *Journal of Biological Chemistry* 1993 **268** 15174–15179. ([https://doi.org/10.1016/S0021-9258\(18\)82452-8](https://doi.org/10.1016/S0021-9258(18)82452-8))
- Roselli-Rehffuss L, Mountjoy KG, Robbins LS, Mortrud MT, Low MJ, Tatro JB, Entwistle ML, Simerly RB & Cone RD. Identification of a receptor for  $\gamma$  melanotropin and other proopiomelanocortin peptides in the hypothalamus and limbic system. *PNAS* 1993 **90** 8856–8860. (<https://doi.org/10.1073/pnas.90.19.8856>)
- Mountjoy KG, Mortrud MT, Low MJ, Simerly RB & Cone RD. Localization of the melanocortin-4 receptor (MC4R) in neuroendocrine and autonomic control circuits in the brain. *Molecular Endocrinology* 1994 **8** 1298–1308. (<https://doi.org/10.1210/mend.8.10.7854347>)
- Tao YX. Mutations in melanocortin-4 receptor and human obesity. *Progress in Molecular Biology and Translational Science* 2009 **88** 173–204. ([https://doi.org/10.1016/S1877-1173\(09\)88006-X](https://doi.org/10.1016/S1877-1173(09)88006-X))
- Tao YX. Mutations in the melanocortin-3 receptor (MC3R) gene: impact on human obesity or adiposity. *Current Opinion in Investigational Drugs* 2010 **11** 1092–1096.
- Yang Z & Tao YX. Mutations in melanocortin-3 receptor gene and human obesity. *Progress in Molecular Biology and Translational Science* 2016 **140** 97–129. (<https://doi.org/10.1016/bs.pmbts.2016.01.002>)
- Huszar D, Lynch CA, Fairchild-Huntress V, Dunmore JH, Fang Q, Berkemeier LR, Gu W, Kesterson RA, Boston BA, Cone RD, *et al.* Targeted disruption of the melanocortin-4 receptor results in obesity in mice. *Cell* 1997 **88** 131–141. ([https://doi.org/10.1016/S0092-8674\(00\)81865-6](https://doi.org/10.1016/S0092-8674(00)81865-6))
- Balthasar N, Dalgaard LT, Lee CE, Yu J, Funahashi H, Williams T, Ferreira M, Tang V, McGovern RA, Kenny CD, *et al.* Divergence of melanocortin pathways in the control of food intake and energy expenditure. *Cell* 2005 **123** 493–505. (<https://doi.org/10.1016/j.cell.2005.08.035>)
- Chen AS, Marsh DJ, Trumbauer ME, Frazier EG, Guan XM, Yu H, Rosenblum CI, Vongs A, Feng Y, Cao L, *et al.* Inactivation of the mouse melanocortin-3 receptor results in increased fat mass and reduced lean body mass. *Nature Genetics* 2000 **26** 97–102. (<https://doi.org/10.1038/79254>)
- Butler AA, Kesterson RA, Khong K, Cullen MJ, Pelleymounter MA, Dekoning J, Baetscher M & Cone RD. A unique metabolic syndrome causes obesity in the melanocortin-3 receptor-deficient mouse. *Endocrinology* 2000 **141** 3518–3521. (<https://doi.org/10.1210/endo.141.9.7791>)
- Zhang Y, Kilroy GE, Henagan TM, Prpic-Uhing V, Richards WG, Bannon AW, Mynatt RL & Gettys TW. Targeted deletion of melanocortin receptor subtypes 3 and 4, but not CART, alters nutrient partitioning and compromises behavioral and metabolic responses to leptin. *FASEB Journal* 2005 **19** 1482–1491. (<https://doi.org/10.1096/fj.05-3851com>)

- 17 Sutton GM, Perez-Tilve D, Nogueiras R, Fang J, Kim JK, Cone RD, Gimble JM, Tschop MH & Butler AA. The melanocortin-3 receptor is required for entrainment to meal intake. *Journal of Neuroscience* 2008 **28** 12946–12955. (<https://doi.org/10.1523/JNEUROSCI.3615-08.2008>)
- 18 Begriche K, Marston OJ, Rossi J, Burke LK, McDonald P, Heisler LK & Butler AA. Melanocortin-3 receptors are involved in adaptation to restricted feeding. *Genes, Brain, and Behavior* 2012 **11** 291–302. (<https://doi.org/10.1111/j.1601-183X.2012.00766.x>)
- 19 Ghamari-Langroudi M, Cakir I, Lippert RN, Sweeney P, Litt MJ, Ellacott KLJ & Cone RD. Regulation of energy rheostasis by the melanocortin-3 receptor. *Science Advances* 2018 **4** eaat0866. (<https://doi.org/10.1126/sciadv.aat0866>)
- 20 Getting SJ, Riffo-Vasquez Y, Pitchford S, Kaneva M, Grieco P, Page CP, Perretti M & Spina D. A role for MC3R in modulating lung inflammation. *Pulmonary Pharmacology and Therapeutics* 2008 **21** 866–873. (<https://doi.org/10.1016/j.pupt.2008.09.004>)
- 21 Getting SJ, Lam CW, Chen AS, Grieco P & Perretti M. Melanocortin 3 receptors control crystal-induced inflammation. *FASEB Journal* 2006 **20** 2234–2241. (<https://doi.org/10.1096/fj.06-6339.com>)
- 22 Chhajlani V. Distribution of cDNA for melanocortin receptor subtypes in human tissues. *Biochemistry and Molecular Biology International* 1996 **38** 73–80.
- 23 Patel HB, Montero-Melendez T, Greco KV & Perretti M. Melanocortin receptors as novel effectors of macrophage responses in inflammation. *Frontiers in Immunology* 2011 **2** 41. (<https://doi.org/10.3389/fimmu.2011.00041>)
- 24 Catania A, Gatti S, Colombo G & Lipton JM. Targeting melanocortin receptors as a novel strategy to control inflammation. *Pharmacological Reviews* 2004 **56** 1–29. (<https://doi.org/10.1124/pr.56.1.1>)
- 25 Getting SJ, Christian HC, Lam CW, Gavins FN, Flower RJ, Schioth HB & Perretti M. Redundancy of a functional melanocortin 1 receptor in the anti-inflammatory actions of melanocortin peptides: studies in the recessive yellow (e/e) mouse suggest an important role for melanocortin 3 receptor. *Journal of Immunology* 2003 **170** 3323–3330. (<https://doi.org/10.4049/jimmunol.170.6.3323>)
- 26 Wang W, Guo DY, Lin YJ & Tao YX. Melanocortin regulation of inflammation. *Frontiers in Endocrinology* 2019 **10** 683. (<https://doi.org/10.3389/fendo.2019.00683>)
- 27 Versteeg DH, Van Bergen P, Adan RA & De Wildt DJ. Melanocortins and cardiovascular regulation. *European Journal of Pharmacology* 1998 **360** 1–14. ([https://doi.org/10.1016/s0014-2999\(98\)00615-3](https://doi.org/10.1016/s0014-2999(98)00615-3))
- 28 Mioni C, Giuliani D, Cainazzo MM, Leone S, Bazzani C, Grieco P, Novellino E, Tomasi A, Bertolini A & Guarini S. Further evidence that melanocortins prevent myocardial reperfusion injury by activating melanocortin MC3 receptors. *European Journal of Pharmacology* 2003 **477** 227–234. ([https://doi.org/10.1016/s0014-2999\(03\)02184-8](https://doi.org/10.1016/s0014-2999(03)02184-8))
- 29 Chandramohan G, Durham N, Sinha S, Norris K & Vaziri ND. Role of  $\gamma$  melanocyte-stimulating hormone-renal melanocortin 3 receptor system in blood pressure regulation in salt-resistant and salt-sensitive rats. *Metabolism: Clinical and Experimental* 2009 **58** 1424–1429. (<https://doi.org/10.1016/j.metabol.2009.04.022>)
- 30 Metherell LA, Chapple JP, Cooray S, David A, Becker C, Ruschendorf F, Naville D, Begeot M, Khoo B, Nurnberg P, *et al.* Mutations in *MRAP*, encoding a new interacting partner of the ACTH receptor, cause familial glucocorticoid deficiency type 2. *Nature Genetics* 2005 **37** 166–170. (<https://doi.org/10.1038/ng1501>)
- 31 Sebag JA & Hinkle PM. Melanocortin-2 receptor accessory protein MRAP forms antiparallel homodimers. *PNAS* 2007 **104** 20244–20249. (<https://doi.org/10.1073/pnas.0708916105>)
- 32 Chan LF, Webb TR, Chung TT, Meimaridou E, Cooray SN, Guasti L, Chapple JP, Egertova M, Elphick MR, Cheetham ME, *et al.* MRAP and MRAP2 are bidirectional regulators of the melanocortin receptor family. *PNAS* 2009 **106** 6146–6151. (<https://doi.org/10.1073/pnas.0809918106>)
- 33 Sebag JA, Zhang C, Hinkle PM, Bradshaw AM & Cone RD. Developmental control of the melanocortin-4 receptor by MRAP2 proteins in zebrafish. *Science* 2013 **341** 278–281. (<https://doi.org/10.1126/science.1232995>)
- 34 Rouault AAJ, Srinivasan DK, Yin TC, Lee AA & Sebag JA. Melanocortin receptor accessory proteins (MRAPs): functions in the melanocortin system and beyond. *Biochimica et Biophysica Acta* 2017 **1864** 2322–2329. (<https://doi.org/10.1016/j.bbdis.2017.05.008>)
- 35 Tao YX. Molecular chaperones and G protein-coupled receptor maturation and pharmacology. *Molecular and Cellular Endocrinology* 2020 **511** 110862. (<https://doi.org/10.1016/j.mce.2020.110862>)
- 36 Asai M, Ramachandrapa S, Joachim M, Shen Y, Zhang R, Nuthalapati N, Ramanathan V, Strohlic DE, Ferket P, Linhart K, *et al.* Loss of function of the melanocortin 2 receptor accessory protein 2 is associated with mammalian obesity. *Science* 2013 **341** 275–278. (<https://doi.org/10.1126/science.1233000>)
- 37 Novoselova TV, Larder R, Rimmington D, Lelliott C, Wynn EH, Gorrigan RJ, Tate PH, Guasti L, Sanger Mouse Genetics Project, O'Rahilly S, *et al.* Loss of *Mrap2* is associated with *Sim1* deficiency and increased circulating cholesterol. *Journal of Endocrinology* 2016 **230** 13–26. (<https://doi.org/10.1530/JOE-16-0057>)
- 38 Zhang J, Li X, Zhou Y, Cui L, Li J, Wu C, Wan Y, Li J & Wang Y. The interaction of MC3R and MC4R with MRAP2, ACTH,  $\alpha$ -MSH and AgRP in chickens. *Journal of Endocrinology* 2017 **234** 155–174. (<https://doi.org/10.1530/JOE-17-0131>)
- 39 Rao YZ, Chen R, Zhang Y & Tao YX. Orange-spotted grouper melanocortin-4 receptor: modulation of signaling by MRAP2. *General and Comparative Endocrinology* 2019 **284** 113234. (<https://doi.org/10.1016/j.ygcen.2019.113234>)
- 40 Tao M, Ji RL, Huang L, Fan SY, Liu T, Liu SJ & Tao YX. Regulation of melanocortin-4 receptor pharmacology by two isoforms of melanocortin receptor accessory protein 2 in topmouth culter (*Culter alburnus*). *Frontiers in Endocrinology* 2020 **11** 538. (<https://doi.org/10.3389/fendo.2020.00538>)
- 41 Wen ZY, Liu T, Qin CJ, Zou YC, Wang J, Li R & Tao YX. MRAP2 interaction with melanocortin-4 receptor in snakehead (*Channa argus*). *Biomolecules* 2021 **11** 481. (<https://doi.org/10.3390/biom11030481>)
- 42 Li L, Xu Y, Zheng J, Kuang Z, Zhang C, Li N, Lin G & Zhang C. Pharmacological modulation of dual melanocortin-4 receptor signaling by melanocortin receptor accessory proteins in the *Xenopus laevis*. *Journal of Cellular Physiology* 2021 **236** 5980–5993. (<https://doi.org/10.1002/jcp.30280>)
- 43 Yang LK, Zhang ZR, Wen HS & Tao YX. Characterization of channel catfish (*Ictalurus punctatus*) melanocortin-3 receptor reveals a potential network in regulation of energy homeostasis. *General and Comparative Endocrinology* 2019 **277** 90–103. (<https://doi.org/10.1016/j.ygcen.2019.03.011>)
- 44 Klovinis J, Haitina T, Ringholm A, Lowgren M, Fridmanis D, Slaidina M, Stier S & Schioth HB. Cloning of two melanocortin (MC) receptors in spiny dogfish: MC3 receptor in cartilaginous fish shows high affinity to ACTH-derived peptides while it has lower preference to  $\gamma$ -MSH. *European Journal of Biochemistry* 2004 **271** 4320–4331. (<https://doi.org/10.1111/j.1432-1033.2004.04374.x>)
- 45 Logan DW, Bryson-Richardson RJ, Taylor MS, Currie P & Jackson IJ. Sequence characterization of teleost fish melanocortin receptors. *Annals of the New York Academy of Sciences* 2003 **994** 319–330. (<https://doi.org/10.1111/j.1749-6632.2003.tb03196.x>)
- 46 Selz Y, Braasch I, Hoffmann C, Schmidt C, Schultheis C, Schartl M & Volff JN. Evolution of melanocortin receptors in teleost fish: the melanocortin type 1 receptor. *Gene* 2007 **401** 114–122. (<https://doi.org/10.1016/j.gene.2007.07.005>)
- 47 Yi TL, Yang LK, Ruan GL, Yang DQ & Tao YX. Melanocortin-4 receptor in swamp eel (*Monopterus albus*): cloning, tissue distribution, and pharmacology. *Gene* 2018 **678** 79–89. (<https://doi.org/10.1016/j.gene.2018.07.056>)



- 48 Rocha A, Godino-Gimeno A & Cerda-Reverter JM. Evolution of proopiomelanocortin. *Vitamins and Hormones* 2019 **111** 1–16. (<https://doi.org/10.1016/bs.vh.2019.05.008>)
- 49 Renquist BJ, Zhang C, Williams SY & Cone RD. Development of an assay for high-throughput energy expenditure monitoring in the zebrafish. *Zebrafish* 2013 **10** 343–352. (<https://doi.org/10.1089/zeb.2012.0841>)
- 50 Sanchez E, Rubio VC, Thompson D, Metz J, Flik G, Millhauser GL & Cerda-Reverter JM. Phosphodiesterase inhibitor-dependent inverse agonism of agouti-related protein on melanocortin 4 receptor in sea bass (*Dicentrarchus labrax*). *American Journal of Physiology: Regulatory, Integrative and Comparative Physiology* 2009 **296** R1293–R1306. (<https://doi.org/10.1152/ajpregu.90948.2008>)
- 51 Li JT, Yang Z, Chen HP, Zhu CH, Deng SP, Li GL & Tao YX. Molecular cloning, tissue distribution, and pharmacological characterization of melanocortin-4 receptor in spotted scat, *Scatophagus argus*. *General and Comparative Endocrinology* 2016 **230–231** 143–152. (<https://doi.org/10.1016/j.ygcen.2016.04.010>)
- 52 Li L, Yang Z, Zhang YP, He S, Liang XF & Tao YX. Molecular cloning, tissue distribution, and pharmacological characterization of melanocortin-4 receptor in grass carp (*Ctenopharyngodon idella*). *Domestic Animal Endocrinology* 2017 **59** 140–151. (<https://doi.org/10.1016/j.domaniend.2016.11.004>)
- 53 Zhang KQ, Hou ZS, Wen HS, Li Y, Qi X, Li WJ & Tao YX. Melanocortin-4 receptor in spotted sea bass, *Lateolabrax maculatus*: cloning, tissue distribution, physiology, and pharmacology. *Frontiers in Endocrinology* 2019 **10** 705. (<https://doi.org/10.3389/fendo.2019.00705>)
- 54 Ji LQ, Rao YZ, Zhang Y, Chen R & Tao YX. Regulation of melanocortin-1 receptor pharmacology by melanocortin receptor accessory protein 2 in orange-spotted grouper (*Epinephelus coioides*). *General and Comparative Endocrinology* 2020 **285** 113291. (<https://doi.org/10.1016/j.ygcen.2019.113291>)
- 55 Chen YY. *Fauna Sinica Osteichthyes Cypriniformes II*. Beijing, China: Science Press, 1998.
- 56 Ren L, Li WH, Qin QB, Dai H, Han FM, Xiao J, Gao X, Cui JL, Wu C, Yan XJ, *et al.* The subgenomes show asymmetric expression of alleles in hybrid lineages of *Megalobrama amblycephala* x *Culter Alburnus*. *Genome Research* 2019 **29** 1805–1815. (<https://doi.org/10.1101/gr.249805.119>)
- 57 Steiner AL, Kipnis DM, Utiger R & Parker C. Radioimmunoassay for the measurement of adenosine 3',5'-cyclic phosphate. *PNAS* 1969 **64** 367–373. (<https://doi.org/10.1073/pnas.64.1.367>)
- 58 Mo XL, Yang R & Tao YX. Functions of transmembrane domain 3 of human melanocortin-4 receptor. *Journal of Molecular Endocrinology* 2012 **49** 221–235. (<https://doi.org/10.1530/JME-12-0162>)
- 59 Tao YX & Segaloff DL. Functional characterization of melanocortin-3 receptor variants identify a loss-of-function mutation involving an amino acid critical for G protein-coupled receptor activation. *Journal of Clinical Endocrinology and Metabolism* 2004 **89** 3936–3942. (<https://doi.org/10.1210/jc.2004-0367>)
- 60 Livak KJ & Schmittgen TD. Analysis of relative gene expression data using real-time quantitative PCR and the 2<sup>-ΔΔCT</sup> method. *Methods* 2001 **25** 402–408. (<https://doi.org/10.1006/meth.2001.1262>)
- 61 Tao YX & Segaloff DL. Functional characterization of melanocortin-4 receptor mutations associated with childhood obesity. *Endocrinology* 2003 **144** 4544–4551. (<https://doi.org/10.1210/en.2003-0524>)
- 62 Chen C & Okayama H. High-efficiency transformation of mammalian cells by plasmid DNA. *Molecular and Cellular Biology* 1987 **7** 2745–2752. (<https://doi.org/10.1128/mcb.7.8.2745-2752.1987>)
- 63 Wang SX, Fan ZC & Tao YX. Functions of acidic transmembrane residues in human melanocortin-3 receptor binding and activation. *Biochemical Pharmacology* 2008 **76** 520–530. (<https://doi.org/10.1016/j.bcp.2008.05.026>)
- 64 Takahashi A, Davis P, Reinick C, Mizusawa K, Sakamoto T & Dores RM. Characterization of melanocortin receptors from stingray *Dasyatis akajei*, a cartilaginous fish. *General and Comparative Endocrinology* 2016 **232** 115–124. (<https://doi.org/10.1016/j.ygcen.2016.03.030>)
- 65 Haitina T, Klovinis J, Andersson J, Fredriksson R, Lagerstrom MC, Larhammar D, Larson ET & Schioth HB. Cloning, tissue distribution, pharmacology and three-dimensional modelling of melanocortin receptors 4 and 5 in rainbow trout suggest close evolutionary relationship of these subtypes. *Biochemical Journal* 2004 **380** 475–486. (<https://doi.org/10.1042/BJ20031934>)
- 66 Klovinis J, Haitina T, Fridmanis D, Kilianova Z, Kapa I, Fredriksson R, Gallo-Payet N & Schioth HB. The melanocortin system in Fugu: determination of POMC/AGRP/MCR gene repertoire and synteny, as well as pharmacology and anatomical distribution of the MCRs. *Molecular Biology and Evolution* 2004 **21** 563–579. (<https://doi.org/10.1093/molbev/msh050>)
- 67 Metz JR, Peters JJ & Flik G. Molecular biology and physiology of the melanocortin system in fish: a review. *General and Comparative Endocrinology* 2006 **148** 150–162. (<https://doi.org/10.1016/j.ygcen.2006.03.001>)
- 68 Kay EI, Botha R, Montgomery JM & Mountjoy KG. hMRAPa increases αMSH-induced hMC1R and hMC3R functional coupling and hMC4R constitutive activity. *Journal of Molecular Endocrinology* 2013 **50** 203–215. (<https://doi.org/10.1530/JME-12-0221>)
- 69 Soletto L, Hernandez-Balfago S, Rocha A, Scheerer P, Kleinau G & Cerda-Reverter JM. Melanocortin receptor accessory protein 2-induced adrenocorticotrophic hormone response of human melanocortin 4 receptor. *Journal of the Endocrine Society* 2019 **3** 314–323. (<https://doi.org/10.1210/je.2018-00370>)
- 70 Josep Agulleiro M, Cortes R, Fernandez-Duran B, Navarro S, Guillot R, Meimaridou E, Clark AJ & Cerda-Reverter JM. Melanocortin 4 receptor becomes an ACTH receptor by coexpression of melanocortin receptor accessory protein 2. *Molecular Endocrinology* 2013 **27** 1934–1945. (<https://doi.org/10.1210/me.2013-1099>)
- 71 Tao YX. Functional characterization of novel melanocortin-3 receptor mutations identified from obese subjects. *Biochimica et Biophysica Acta* 2007 **1772** 1167–1174. (<https://doi.org/10.1016/j.bbadis.2007.09.002>)
- 72 Tao YX, Huang H, Wang ZQ, Yang F, Williams JN & Nikiforovich GV. Constitutive activity of neural melanocortin receptors. *Methods in Enzymology* 2010 **484** 267–279. (<https://doi.org/10.1016/B978-0-12-381298-8.00014-9>)
- 73 Tao YX. Constitutive activation of G protein-coupled receptors and diseases: insights into mechanism of activation and therapeutics. *Pharmacology and Therapeutics* 2008 **120** 129–148. (<https://doi.org/10.1016/j.pharmthera.2008.07.005>)
- 74 Srinivasan S, Lubrano-Berthelie C, Govaerts C, Picard F, Santiago P, Conklin BR & Vaisse C. Constitutive activity of the melanocortin-4 receptor is maintained by its N-terminal domain and plays a role in energy homeostasis in humans. *Journal of Clinical Investigation* 2004 **114** 1158–1164. (<https://doi.org/10.1172/JCI21927>)
- 75 Zhang C, Forlano PM & Cone RD. AgRP and POMC neurons are hypophysiotropic and coordinately regulate multiple endocrine axes in a larval teleost. *Cell Metabolism* 2012 **15** 256–264. (<https://doi.org/10.1016/j.cmet.2011.12.014>)

Received in final form 12 October 2021

Accepted 22 October 2021

Accepted Manuscript published online 22 October 2021